Geological Quarterly, 2021, 65: 19
DOI: http://dx.doi.org/10.7306/gq.1587

Occurrences and characterization of alunite group minerals from the Lece-Radan Oligo-Miocene volcanic complex (Serbia)

Pavle TANČIĆ[1], Darko SPAHIĆ[1, *], Dragan JOVANOVIĆ[1], Aleksandra ĆIRIĆ[1], Maja POZNANOVIĆ-SPAHIĆ[1] and Nenad VASIĆ[1]

[1] Geological Survey of Serbia, Rovinjska 12, 11000 Belgrade, Serbia.

Tančić, P., Spahić, D., Jovanović, D., Ćirić, A., Poznanović-Spahić, M., Vasić, N., 2021. Occurrences and characterization of alunite group minerals from the Lece-Radan Oligo-Miocene volcanic complex (Serbia). Geological Quarterly, 2021, 65: 19, doi: 10.7306/gq.1587

Associate Editor: Tomasz Bajda

The Lece-Radan area of the Oligo-Miocene magmatic complex (former Tethyan active margin, southern Serbia) contains more or less altered volcanic and/or pyroclastic rocks of predominant andesitic, andesitic-dacitic, to dacitic composition. Alteration seen at exposures varies in type and intensity. Samples with documented alunitization were collected from hydrothermally altered zones embedded within local geological units of Oligo-Miocene age. Mineralogical-chemical study has confirmed for the first time the presence of alunite group minerals (thirty-one occurrences) in this area. The minerals of the alunite group described exhibit different compositions that are remarkably consistent with both different alteration types and host lithologies. Six samples characterized in detail show the following solid solutions: $Alu_{52}Nal_{43}Sch_5$, $Alu_{48}Nal_{40}Sch_{12}$, $Nal_{48}Alu_{35}Sch_{17}$, $Nal_{44}Alu_{35}Sch_{21}$, $Alu_{36}Sch_{33}Nal_{31}$ and $Sch_{46}Alu_{27}Nal_{27}$ (Alu, Nal and Sch refer to alunite, natroalunite and schlossmacherite, respectively). The cross-cutting alunite-bearing fracture pattern and its density indicate a high-sulphidation epithermal palaeoenvironment. The alunite discovery is consistent with the structural setting (fracture frequency) emphasizing its dominant role in controlling the local mineralization.

Key words: Lece-Radan volcanic complex, alunite group minerals, high-sulphidation epithermal environment, structural factor, Vardar Zone, Serbo-Macedonian metallogenic province.

INTRODUCTION

Epithermal-type rock alteration associated with upwardly-welling upper-crustal volcanic intrusions has often been referred to as “alunite-kaolinite” or “acid-sulphate” ores. Economically viable epithermal ore deposits commonly form at a shallow depth above lithospheric-scale plate margins, as deep as 1 to 2 km, indicating a temperature range of <150 to ~300°C (White and Hedenquist, 1995). Such shallow crustal levels allow rapid exhumation, post-hydrothermal weathering, and erosion of highly fractured, porous and permeable alteration zones, such that these often gold-bearing assemblies are rarely exposed. Advanced argillic alteration contributes to the total destruction of primary minerals, leaving an insoluble residue of quartz, clays (kaolinite or pyrophyllite), aluminum oxyhydroxides (diaspore) and, importantly, the telltale alunite mineral group (the so-called “leached cap assemblage”; Tosdal et al., 2009).

The alunite supergroup consists of more than 40 mineral species with the general formula:

$$DG_3(TX_4)_2X'_6$$

where: *D* is occupied by Na, K, Rb, Ag, Tl, NH_4, H_3O, vacancies, Ca, Sr, Ba, Pb, Hg, Ce, La, Nd, Bi, and Th ions; *G* is typically Cu^{2+}, Zn^{2+}, Mg, Al^{3+}, Fe^{3+}, V^{3+}, Cr^{3+}, Ga and Sn^{4+}; *T* is S^{6+}, Cr^{6+}, As^{5+}, P^{5+}, Sb or Si; and *X* is O, (OH), (H_2O) and F (Stoffregen et al., 2000; Bayliss, 2010).

The alunite subgroup, as one part of the alunite supergroup, is characterized by $(SO_4)_2$-dominant minerals, i.e., with the general formula $AB_3(SO_4)_2(OH)_6$, where the *A* site is usually occupied by monovalent cations (K^+, Na^+, H_3O^+ and NH_4^+), and the *B* site contains Al^{3+} and Fe^{3+}. The end members are: alunite $KAl_3(SO_4)_2(OH)_6$, jarosite $KFe_3(SO_4)_2(OH)_6$, natroalunite $NaAl_3(SO_4)_2(OH)_6$, natrojarosite $NaFe_3(SO_4)_2(OH)_6$, ammonioalunite $(NH_4)Al_3(SO_4)_2(OH)_6$, ammoniojarosite $(NH_4)Fe_3(SO_4)_2(OH)_6$, schlossmacherite $(H_3O, Ca)Al_3(SO_4)_2(OH)_6$, hydronium jarosite $(H_3O)Fe_3(SO_4)_2(OH)_6$, etc. The alunite-natroalunite and jarosite-natrojarosite solid-solution series are by far the most abundant naturally occurring species of the alunite supergroup.

* Corresponding author, e-mail: darkogeo2002@hotmail.com
Received: October 24, 2020; accepted: February 11, 2021; first published online: April 2 , 2021

Alunites were first discovered in Serbia at the Majdan locality in Boljetin near Kosovska Mitrovica (Tućan, 1938). Ilić (1961) studied a single sample from this locality using X-ray powder diffraction (hereinafter XRPD) and chemical methods. The unit cell dimensions were characterized, showing the sample to be a mixture of alunite (in which a small part of K was replaced by Na) and jarosite. Joksimović (1970) documented quartz-alunite rocks at the Kopaonik Mt. area near Lukovska Banja. Vasić (1986) explored alunites at Biočin near Raška, with a single sample from the Veliki Bukovik locality being studied with differential thermal analysis (DTA), thermogravimetric analysis (TGA), and chemical analysis and determined as pure alunite. However, Tančić and Janežić (2004) further studied this sample by XRPD and suggested that it is a mixture of major alunite and natroalunite in about equal contents, with minor jarosite, quartz, and feldspars. The unit cell dimensions of the alunite, natroalunite, and jarosite together with the chemical composition were used for the characterization of the crystallochemical formulae of the alunite and natroalunite. Alunite mineralization has also been documented in other magmatic provinces Bor, Majdanpek, and Veliki Krivelj (Janković, 1990).

A shallow epithermal volcanic palaeoenvironment is described near the Lece ore-bearing site in southern Serbia (Stajević, 2004; Fig. 1A, B), the Lece-Radan volcanic complex (Jelenković et al., 2008; Fig. 1B), related to Oligo-Miocene extension, which is just partially undergoing exploration. Details of the mineralogy, (ore) geology, and of the tectonic environment that produced relatively young volcanism, are not fully understood. As the presence of alunite proved to be informative regarding the high-sulphidation hydrothermal conditions, this paper investigates the epithermal environment *via* documenting the alunite group and/or other marker minerals. It documents the first discovery of alunite mineralization in the Lece-Radan volcanic complex in the context of the enclosing rocks and their observed hydrothermal alteration, the mineral compositions being analysed by petrographic, XRPD, chemical, and ore microscopy methods.

GEOGRAPHIC-GEOLOGICAL OUTLINE AND METALLOGENIC SETTING

The Lece-Radan calc-alkaline volcanic complex or Lece district (Janković, 1977) is located in a mountainous region of southeastern Europe, southern Serbia (Fig. 1A, B), and covers an area of ~720 km^2. This area lies in the core of the polyorogenic Variscan-Alpine amalgamation of former Yugoslavia and Serbia (Fig. 1C). The regional tectonostratigraphic assembly of former Yugoslavia is represented by a deformed rock amalgamation shaped by the Phanerozoic interaction of European Gondwana-derived crust and intervening oceans. The area of central-southern Serbia (Fig. 1B) hosts Jurassic Neotethyan vestiges of ophiolite-bearing oceanic crust (Vardar accretionary wedge, Vardar Zone) and the overriding Serbo-Macedonian Unit (alternatively referred to as the "Serbo-Macedonian Massif"; Dimitrijević, 1997; Schmid et al., 2020; Spahić and Gaudenyi, 2019; *sensu* Spahić and Gaudenyi, 2020; Fig. 1C). Consequently, the Lece-Radan magmatic and sedimentary assemblage is located above an intersecting deep-seated lithospheric-scale crustal fault (Vukašinović, 1973) connected to the nearby Neotethyan palaeosuture (Dimitrijević and Grubić, 1977; Janković, 1977; Dimitrijević, 1997; Fig. 1C). This Late Cretaceous–Paleogene convergent boundary seems to have been reactivated by Neoalpine Late Oligocene inversion marked by widespread extensional motions of the local microplates. The Lece-Radan volcanic complex is positioned on top of two principal, formerly converging, first-order geotectonic units: the Serbo-Macedonian Unit and the ophiolite-bearing Vardar Zone in the west (Fig. 1C). This distinctive lithospheric-scale interface area can be designated as the "Internal Vardar Zone" (Dimitrijević, 1997; Fig. 1C) or the very western margin of the Serbo-Macedonian Unit. The "Internal Vardar Zone" in the vicinity of the Lece-Radan complex is characterized by a Lower Cretaceous megasequence, including the nearby ophiolite-bearing oceanic vestiges of the West Vardar Zone and Late Cretaceous turbidites (Dimitrijević, 1997). The complex itself is accommodated within the western margin of the Serbo-Macedonian Unit (Fig. 1A). Apparently, the Late Cretaceous-Paleogene Neotethyan palaeosuture underwent significant extensional reactivation and crustal thinning during the Neoalpine stage. The Neoalpine extensional reactivation of the fossil Neotethyan convergent plate margin allowed recurrent Late Oligocene-Miocene volcanic activity (the "volcanic climax" of Janković, 1977). The changeover of the regional tectonic forces yielded the Neoalpine stage marked by the Early Miocene – Ottnangian depositional onset. At the regional scale (former Yugoslavia), the imprints of regionally widespread Neogene extension and subsidence are (i) the landlocked Pannonian Basin and (ii) its southern extension/bays (to the south of Belgrade; Fig. 1) reaching the modern-day Južna Morava River (Marović et al., 2007). As regards the Lece-Radan vicinity, however, it seems that the extension took place slightly earlier (probably along the intersecting inherited Tupale dislocation; Dimitrijević, 1997). Thus, the initial extension-driven volcano-sedimentary system is of Late Oligocene age (Malešević et al., 1979; Vukanović et al., 1982).

The Lece-Radan area investigated comprises Neogene volcanic rocks, which includes the Upper Oligocene volcano-sedimentary unit. Four principal magmatic and sedimentary sequences occupy the wider area investigated, while the two main events occurred during the Late Oligocene-Miocene (Malešević et al., 1979; Vukanović et al., 1982). The Lece-Radan volcanic complex is mainly represented by tuffs, volcanic breccias, andesites, quartz latites, and secondary quartzites (Fig. 2). A small peripheral area includes conglomerates, sandstones, and marls with limestone. The rocks underwent hydrothermal alteration of contrasting intensities.

METALLOGENIC ZONING

As noted earlier, epithermal ore deposits form at shallow depths (White and Hedenquist, 1995). Epithermal Au deposits are a type of lode deposit bearing economic concentrations of Au (±Ag and base metals; Taylor, 2007). Epithermal deposits may have a similar age to their host rocks, in particular when they are of volcanic origin or (typically) are younger than their host rock. The Lece-Radan volcanic complex is characterized by high and low sulphidation epithermal gold mineralization, being a segment of the first-order Serbo-Macedonian metallogenetic unit (Jelenković et al., 2008). The Serbo-Macedonian metallogenic province occupies the central part of Serbia, covering terrains of the Vardar Zone, accommodated between the underlying eastern part of the Dinarides and the crystalline Serbo-Macedonian Unit (Fig. 1C). The magmatic ore-bearing complex investigated belongs to the Lece-Halkidiki metallogenic zone, Lece district (Janković, 1977) or Lece ore field (Jelenković et al., 2008). The principal minerals are galena, sphalerite, pyrite, and Au, documented in andesites and quartz veins. The Lece ore-bearing complex, which is to the south-east of the investigated Lece-Radan area (Fig. 2; see also Stajević, 2004), is already at the exploration stage with appropriate processing

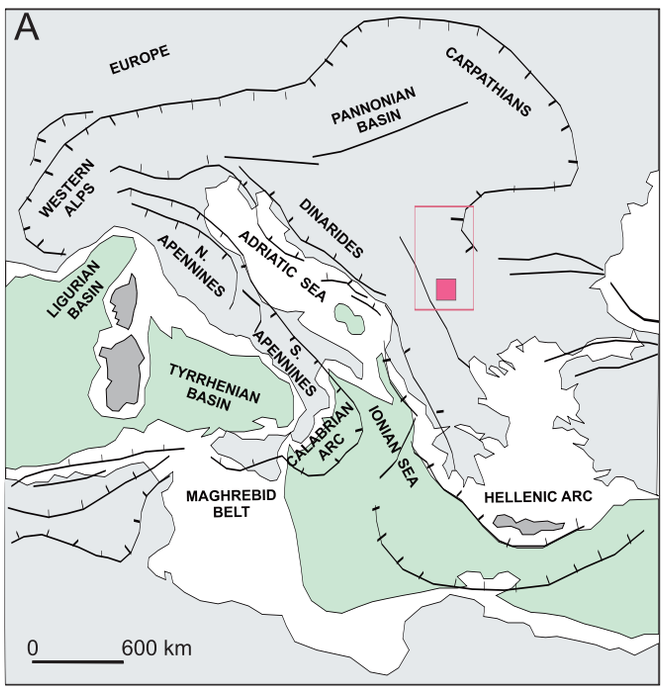

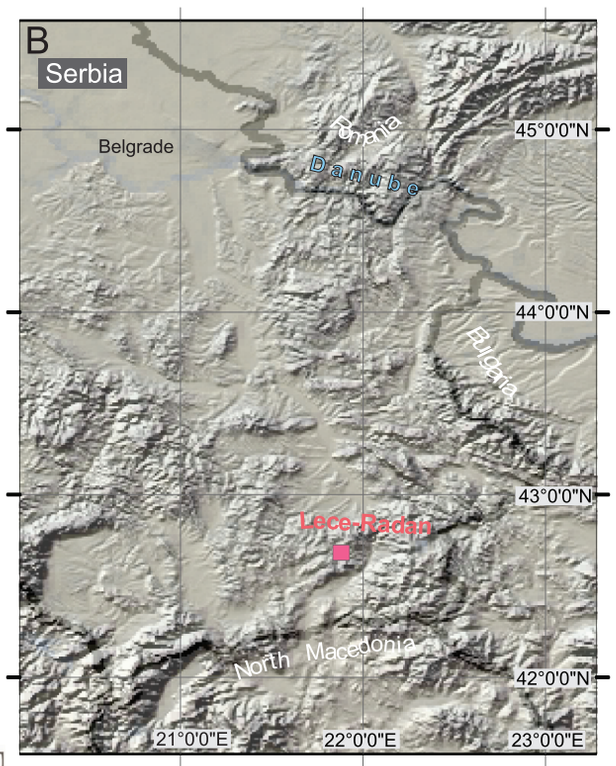

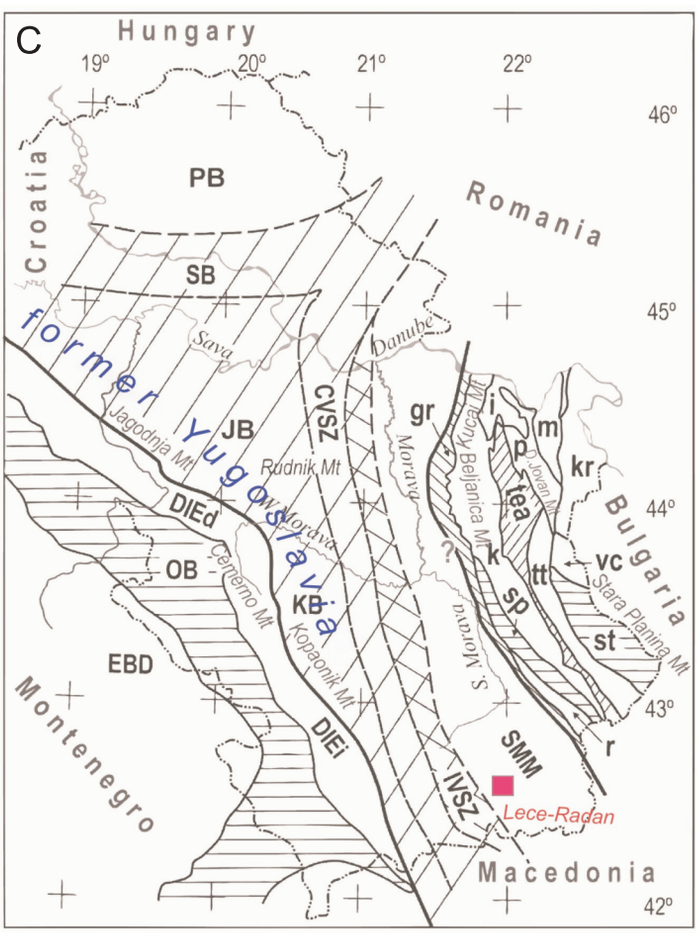

Fig. 1A – principal large-scale structural units of the Alpine orogeny in Central Europe (Lece-Radan area marked in red); B – relief map of the wider area investigated (eastern former Yugoslavia) with the position of the Lece-Radan complex; C – principal tectonic units of Serbia after Dimitrijević (1997), also in Jelenković et al. (2008)

Dinarides: EBD – East Bosnian-Durmitor, OB – Ophiolite Belt, DIE – Drina Ivanjica Element (d – Drina Block, i – Ivanjica Block); Vardar zone, External Vardar Subzone: SB – Srem Block, JB – Jadar Block, KB – Kopaonik Block; CVSZ – Central Vardar Subzone; IVSZ – Internal Vardar Subzone; SMM – Serbo-Macedonian Massif: Carpatho-Balkanides: gr – Gornjak-Ravanica Zone, r – Ruj Zone, sp – Stara Planina Zone, k – Kučaj Zone, i – Liškova (Homolje) metamorphites, tea – Timok eruptive area, tt – Tupižnica-Tepoš Zone, p – Poreč Unit, m – Miroč Zone, st – Suva Planina, kr – Krajina Unit; PB – Pannonian Basin; the area investigated belongs to the Internal Vardar Subzone (IVSZ)

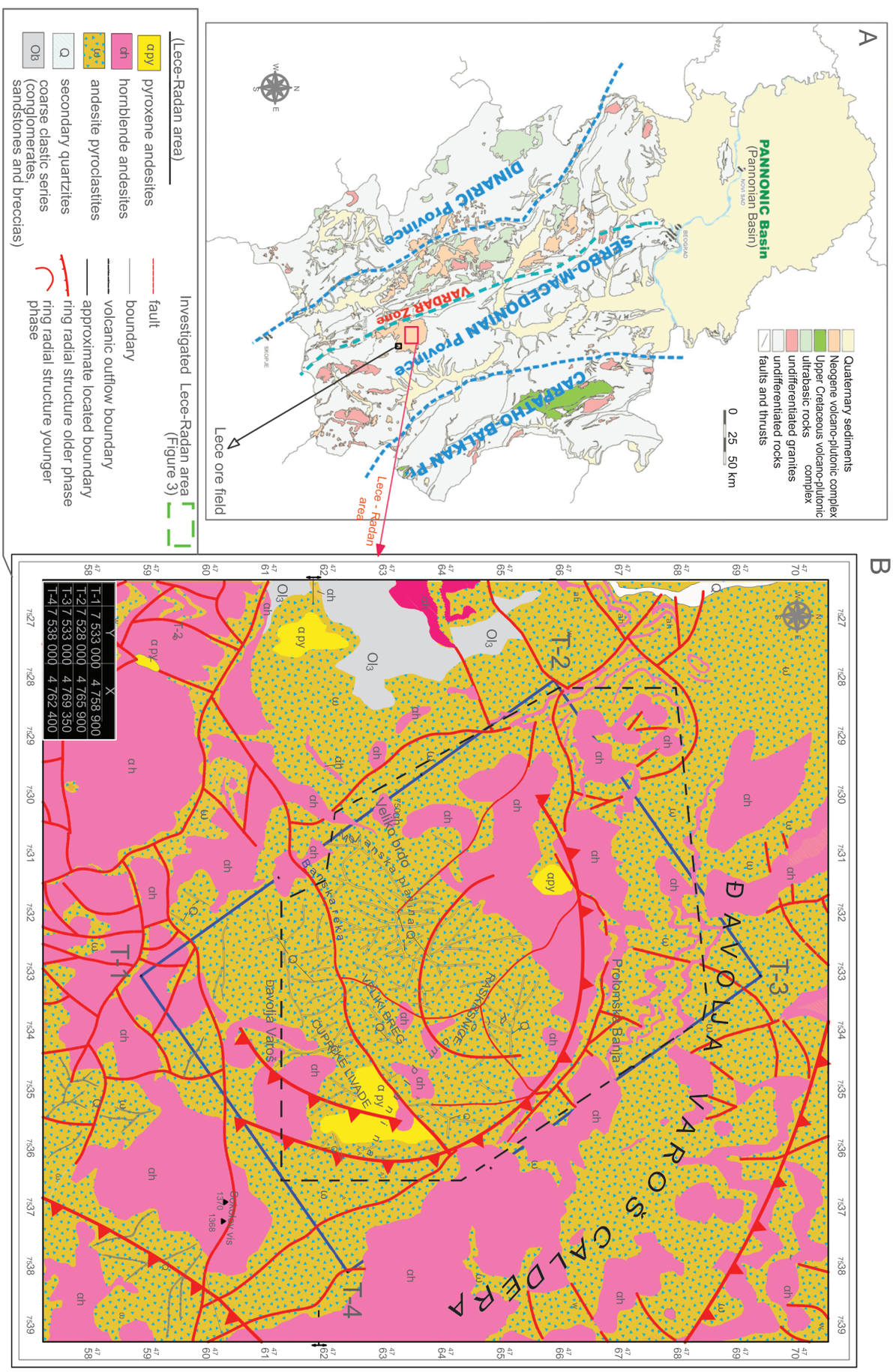

Fig. 2A – simplified geological map of Serbia showing the main structural and metallogenic provinces (Monthel et al., 2002; Jelenković et al., 2008) with the Lece-Radan area marked; B – structural-geological map showing the position of the part of the terrain investigated (T1-T4)

capacities (Cu, Pb, and Zn). The Lece-Halkidiki metallogenic zone is the ore-bearing area of higher exploration potential with well-defined control factors. Its spatial position, and the factors that led to the origin of individual deposits of gold, have been well-constrained (Jelenković, 1998).

MATERIALS AND METHODS

The surface exploration Lece-Radan area covers ~53 km^2 (Fig. 2). Sampling for laboratory tests was conducted by collecting rocks with macroscopically visible marks of hydrothermal alteration within the largest "Đavolja Varoš" caldera. Regarding the variances of the mineral occurrences observed, particularly those of the alunite group, the whole set of exposed hydrothermally altered rocks was included in sampling/alteration mapping. The sampling network and its density are in accordance with the type and the intensity of exposed hydrothermal alteration (Fig. 3).

Thin-sections from 77 samples underwent petrographic study using a *Carl Zeiss* transmitted light microscope. 180 samples for XRPD analysis were first dried at 105°C and powdered to >~0.07 mm by plate mill. The analysis was performed on a *PHILIPS* powder automatic X-ray diffractometer, model *PW-1710*. The long-focus (LFF) Cu-anode (U = 40 kV and I = 30 mA), with monochromatic Kλ1 radiation (λ = 1.54060Å) and Xe proportional counter, was used. Diffraction data were collected in the 4–65° 2θ angle range, with 0.25 s/step counting time on every 0.02°. For the measurement of angle positions of the diffraction maxima and their intensities, *PW-1877* software was used. The precision of the diffractometer was controlled before and after the experiment with a metallic Si powder standard. Calculations of unit cell dimensions were computed by using least-square unit cell refinement (*LSUCRI*) software (Garvey, 1987).

Finally, six samples with a major alunite-group content were chemically analysed according to their total decomposition:

a – by using a combination of HF/$HClO_4$ acids (in the case of Na and K);

b – by fusion with Na_2CO_3 (other elements).

Au was observed after acid digestion (Aqua Regia) and MIBK (isobutyl methyl ketone) extraction. The contents of Na, K, Au, Fe, Ca, and Mg were determined using a *PERKIN ELMER 6500 AAS* (Atomic Absorption Spectrophotometer), while Si, Al, and S were measured by using a gravimetric method. Ferro (Fe^{2+}) contents were characterized after acid digestion (H_2SO_4 1:1 solution and HF) in an inert atmosphere by a volumetric method (0.01M $KMnO_4$). Loss of ignition was measured after heating at 250 (LOI^-) and 1000°C (LOI^+). H_2O^+ contents were calculated indirectly by deduction of the SO_3 values from the characterized LOI^+ contents. An *EJKELKAMP* multicomponent pH-meter measured the pH values. These samples were also additionally analysed by ore microscopy, using a reflected light *Carl Zeiss* microscope on polished sections.

RESULTS

LITHOGEOCHEMICAL PROSPECTING: HOST ROCKS AND ALTERATIONS

The host rocks and alteration mineral assemblages of the Lece-Radan Massif were mapped and sampled during staged field-based lithogeochemical prospecting. Andesites represent the main volcanic bodies exposed within the area investigated, though andesitic subvolcanic intrusions were difficult to distinguish in the field, as they underwent intense hydrothermal activity obscuring their early relationships. The hydrothermal changes in the andesites are very pronounced, in particular within the central and southern parts of the complex investigated, marked by the products of silicification, chloritization, and occasionally K-feldspathization, and tourmalinization inclusive of secondary zeolitization (north of the Prolomska Reka). The hydrothermal rock changes observed are characterized primarily by silicification with limonitization of lesser intensity. Andesite tuffs are rarely exposed in the field; scarce exposures show pronounced stratification. The thickness of the tuffs (outcrop scale) is >100 m (Mejanske Planine; Fig. 4A). The products of intense hydrothermal alteration of the tuff (silicification, argillization, and limonitization) are widely distributed. Andesitic volcanic agglomerates and breccias occur in the form of lenticular interlayers, 10 to 50 m thick, within andesitic units. These rocks consist of small andesitic fragments in a tuff-bearing matrix. Agglomerates and breccias are hydrothermally altered, silicified, argillized, and mildly limonitized (Fig. 4B). Hornblende andesites are abundant, being exposed within the andesite complex near Banjska Reka. They are composed of phenocrystals of plagioclase, hornblende, with lesser amounts of pyroxene and accessory apatite, zircon, and opaque metallic minerals (mainly pyrite). The initial composition of the rocks has changed significantly; the assemblage has rarely preserved the original syn-emplacement post-consolidation fabric. Less frequent hornblende andesites build outflows (Banjska Reka, Mejanske Planine) and sub-volcanic intrusions (Veliko Brdo, Sakovski Lazovi, and Raskrsnice). Andesites represent a series of andesitic rocks, with variable quartz content transitioning into hornblende-pyroxene dacites (with increased biotite content into hornblende-pyroxene-biotite andesites with quartz). These rocks are significantly hydrothermally altered between the locations Banjska Reka and Mejanske Planine (silicified, argillized, and partially mineralized; Fig. 4C). In some places, chloritization is the most pronounced, occurring along these transition zones.

Argillization is the most intensive kind of rock alteration observed. The primary rock properties are often completely altered. Because of its soft, clay-rich nature, the host rock cannot be properly observed macroscopically. The colours are off-white or grey-white. There is a gradual transition from less altered to relatively unaltered rocks. The Žute Bare locality (Fig. 4D) exposes argillized rocks that are well-compacted. The rocks are mostly porous (honeycomb, spongy) or filled with reddish-pink or fine-grained reddish material. Silicification frequently occurs in the form of a fine-grained matrix of the rocks. Quartz reefs are less frequent; these can be observed in the field as elements of local relief, e.g., as elevated ridges, being extremely silicified and partially argillized. At the locality of Velika Livada, they form a clearly visible "protruding" local relief, distinctly silicified, exposed as ridges and very argillized parts of the terrain, locally of breccia-like appearance (Fig. 4E). These ridges seem to be exposed along specific directions, with silicification reflected by the presence of fine-grained to medium-grained secondary quartz. These "ridge-zones" extend NE–SW, their lengths ranging from 12 to 75 m, their widths being ~25 m. In some segments of a zone, rocks are dismembered, destroyed at zone tips, wedge-shaped, and disappear beneath the surrounding surface topography of the terrain. Extremely hard rocks, porous, with empty cavities or occasionally filled with fine-grained material, characterize these zones. Limonitization (Fig. 4F) is relatively common and though varying greatly in occurrence and intensity. At some locations, limonitization occurs in the form of limonitized ferro-magnesium and iron minerals, primarily pyrite, and is often a

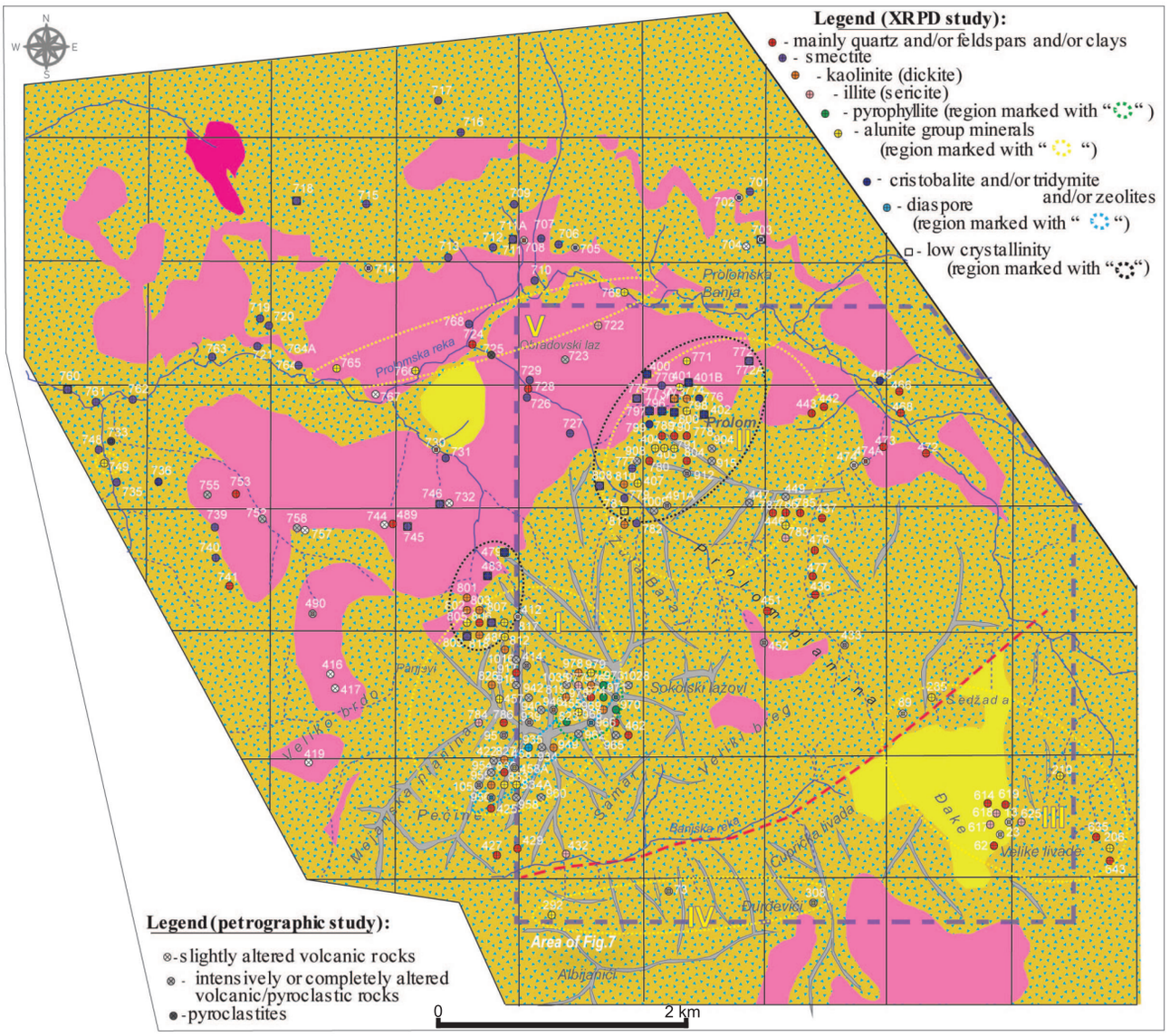

Fig. 3. Rocks and minerals determined from sampling points exclusively within the selected area at Figure 2B (black dashed lines)

Symbols in circles denote study method applied: "×" – petrographic, "+" – XRPD; following regions-zones with recorded alunite group minerals are classified as: I – Žuta Bara (between Žuta Bara, Samar, and Pećine and Panjevi at Mejanske Planine), II – Prolom (between Prolom, Raskrsnice and Žuta Bara), III – Đake (between Sedžada and Velike Livade), IV – Banjska Reka (between Banjska Reka, Đurđevići and Albijanići); V – Prolomska Reka

consequence of external agents (weathering). Limonitization occurs exclusively in certain parts of the rock volume. Sericitization, chloritization (Fig. 4G), and hematitization are less frequent. Several regions of hydrothermally altered rocks were also recorded, which may be relevant in terms of the possible occurrence of alunite mineralization. These are Žuta Bara (Fig. 4H), Prolom, Mejanske Planine, Samar, Đake, Đurđevići, Albijanići, and the region of Prolomska Reka.

PETROGRAPHIC STUDY

The petrographic study focused on the mineral composition, fabric elements (structural and textural features) together with alteration patterns seen in thin-section. The samples collected (Fig. 3) represent altered volcanic and/or pyroclastic rocks of predominantly andesitic, andesitic-dacitic, to dacitic composition (the level of alteration varies from low to high intensity). The following rock types were identified:

1) Slightly altered volcanic rocks:
- andesites (hornblende, hornblende-pyroxene and/or pyroxene andesites) in samples 13, 416, 417, 419, 474, 702, 703, 705, 714, 730, 732, 744, 757 and 767;
- andesites-dacites (samples 89, 242, 266, 276, 282, 317, 412, 704 and 708);
- dacites (samples 21, 23, 84 and 91).

The rock groundmass is mostly hypocrystalline (with a volcanic glass residuum) with the exception of samples 21, 23, 64, 73, 84, 91, 201 and 225 that have a holocrystalline groundmass;

2) Intensely or completely altered volcanic/pyroclastic rocks, most probably of the same primary mineral composition as the volcanic rocks:

- andesitic? (samples 64, 414, 433, 447, 449, 452, 458, 461, 490, 491A, 752, 755, 758, 904, 908, 912, 915, 940, 960, 968, 1016, 1035 and 1050);
- andesitic-dacitic? (samples 73, 158, 201, 225, 265, 308, 422, 455, 723, 916, 926, 934, 939, 942, 946, 951, 954, 956, 958, 962, 965, 971, 1009 and 1028);

3) Pyroclastic rocks (rarely identified; samples 3, 725 and 733), mostly of litho-crystaloclastic texture (lithic to crystal tuff).

Almost the entire set of samples can be characterized by mild to almost complete rock alteration. The recorded alterations are argillization, silicification, sericitization, ±alunitization?, ±prehnitization? of felsic constituents (feldspars) and/or groundmass, and opacitization, chloritization and limonitization of mafic minerals (pyroxene/amphibole/biotite). Minor occurrences of carbonatization and epidotization were occasionally noticed. The alteration types listed above may have often led to a complete change of the primary mineral composition and of rock fabric. Well-preserved elements of primary rock fabric are relatively rare, and a volcanic or pyroclastic origin cannot be unambiguously determined.

XRPD STUDY

The XRPD method enables qualitative and semi-quantitative (determined by relative intensity ratio) mineral compositions of the samples to be determined (Fig. 3; Appendix 1*). The results indicate that quartz (Q, SiO_2), the feldspar group (F) and the clay group (Cl) are the most abundant minerals, present in the great majority of samples analysed (139, 102, and 76 occurrences, respectively).

Although clays occur quite frequently as a mixture of several different minerals within this group, many samples allow their specific determination, e.g., smectite (Sm), kaolinite-dickite (K), pyrophyllite (P), illite-sericite (I), and chlorites (Ch). Smectite is associated with cristobalite, tridymite, and feldspars. It is the major mineral in twelve and minor in thirty-six samples. Kaolinite (and/or dickite) is associated with quartz, cristobalite, alunite group minerals, tridymite and feldspars (as major component in six samples: 401, 457, 771, 773, 774 and 826; and a minor one in 22 samples: 485, 801–803, 805, 810–812, 818, 819, 827, 833, 946, 949, 955, 956, 969, 970, 974, 976, 978, and 979). Illite-sericite occurs in association with quartz and feldspars, and it is represented as minor in ten samples: 432, 617, 618, 625, 722, 783, 784, 791, 951, and 977. Pyrophyllite is identified in several samples (834A, 970, 971, 973, 974, and 979), mostly as a minor component, usually associated with quartz, diaspore, and alunite group minerals. This mineral is highly abundant exclusively in sample 823. Chlorites as minor components were identified exclusively in sample 969.

Alunite group minerals were identified in 31 samples, commonly occurring in an assemblage with quartz, clays, and feldspars. The preliminary identification takes into account the observed *d*-values as alunite (A), natroalunite (NA), jarosite (J), and natrojarosite (NJ). These are major components in samples 401 (A); and 403, 404, 455, 457 and 458A (NA), and minor ones in samples 13, 23, 89, 206, 210, 285, 749, 765, 766, 769 and 771 (A); 485, 781, 805, 833, 834A and 979 (NA); 73, 292, 308, 446, 791, 798 and 817 (J); and 407 (NJ).

Cristobalite (abbreviated by C, SiO_2) occurs mostly in association with quartz, feldspars, tridymite, smectite, and kaolinite. It was identified as a major mineral in samples 401B, 402, 479, 483, 703, 711, 711A, 712, 715, 736, 746, 760, 770, 772–776, 781, 796–800 and 808, and a minor component of samples 702, 718, 735, 739 and 809. Tridymite (T, SiO_2) was identified as a major mineral in samples 401, 715, 718, 733, 745, 760, 771, and 809; and as a minor one within samples 400, 465, 703, 709, 716, and 749.

Amphiboles (Am) were identified mostly as a minor mineral in samples 473, 701, 702, 705, 707, 713, 736, 739–741, 753 and 764. Among minor carbonates, calcite (Ca, $CaCO_3$) occurs in samples 710, 720, 728, 730, 733, and 764; rhodochrosite (R, $MnCO_3$) is documented in samples 706, 709, 720, 721, 727, and 753; and siderite (S, $FeCO_3$) only in sample 720. Zeolites (Z) are characterized as being of the clinoptilolite-heulandite type, identified exclusively in a few samples, as a major component in sample 736, and as minor part of samples 308 and 739. Diaspore [D, α-AlO(OH)] was detected as a minor mineral in samples 282, 823, 935, 956, 968, 971, 973, and 974. Among other minor minerals, hematite (H, α-Fe_2O_3) was identified in samples 308 and 443; goethite [G, α-FeO(OH)] exclusively in sample 211; apatite [Ap, $Ca_5(PO_4)_3(F,Cl,OH)$] in sample 206; pyrite (Py, FeS_2) in sample 308; and graphite (Gr, C-carbon) in samples 709 and 721. The presence of some mineral species (labeled as "?") cannot be unequivocally demonstrated, because of their minor contents and the overlap of the diffraction reflections with other minerals. Therefore, these data should be taken into account with some caution.

Finally, we emphasize that 22 samples are characterized as of low crystallinity (hereinafter LC) degree: 400, 401B, 402, 479, 483, 703, 711A, 718, 745, 746, 760, 772, 772A, 773, 775, 781, 796, 797, 800 and 807–809. These samples are comprised mostly of cristobalite, smectite, and tridymite. The LC may be attributed to the presence of some amorphous phase(s), such as volcanic glass or opal, which could not be detected by XRPD. Nevertheless, the petrographic results show that LC accounts for the previously determined hypocrystalline rock groundmass, which includes a glass residuum.

CHARACTERIZATION OF THE ALUNITE GROUP MINERALS

The crystal structure of alunite and jarosite was initially determined by Hendricks (1937) in the trigonal $R\bar{3}m$ space group and later revised by Wang et al. (1965) and Menchetti and Sabelli (1976). Brophy et al. (1962), Parker (1962), Brophy and Sheridan (1965), Stoffregen and Alpers (1992), including Morrison et al. (2018) studied solid solutions between the end members, and the effects of ionic substitutions to their crystallographic axes. With the goal to reach greater accuracy and lower error levels, unit cell dimensions of minerals (those belonging to the alunite group) are calculated exclusively from samples in which the alunite group represents a major component (401, 403, 404, 455, 457, and 458A; Appendix 1 and Table 1).

* Supplementary data associated with this article can be found, in the online version, at doi: 10.7306/gq.1587

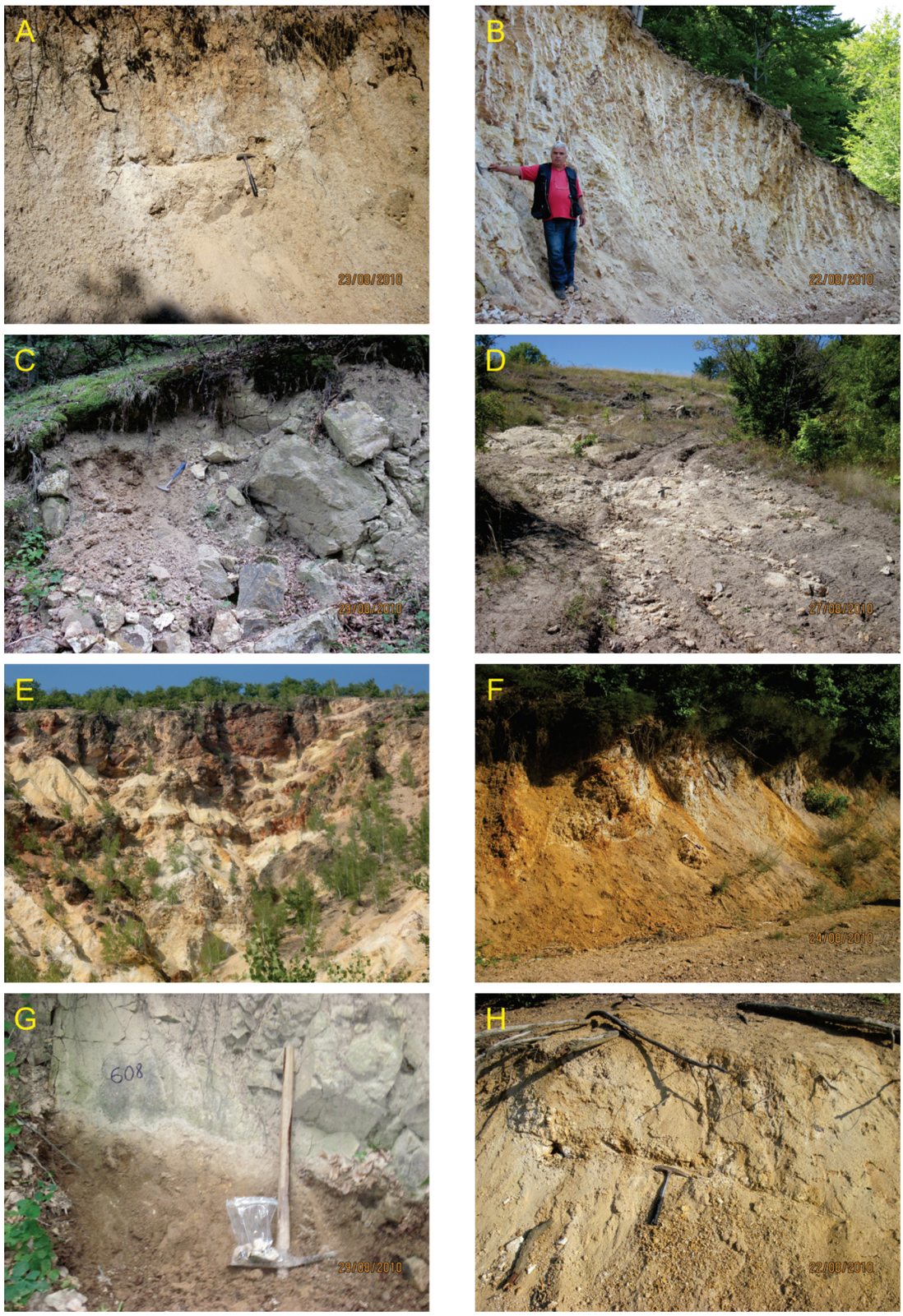

Fig. 4A – andesitic tuff (Mejanske Planine); B – limonitized and argillized andesitic agglomerates (Mejanske Planine); C – weakly altered andesites (Banjska Reka); D – argillization (Žute Bare); E – quartz reefs (Velike Livade-Veliki Breg); F – limonitization (Samari); G – chloritization (Sedžada); H – possible alunitization (Žute Bare)

Table 1

Calculated unit cell dimensions of alunite group minerals

No	a_0 (Å)	c_0 (Å)	V_0 (Å3)	c_0/a_0	1	2	3	4	Average
401	6.971(3)	17.00(1)	715.5(6)	2.439	48	52	59	39	50
403	6.983(2)	16.800(9)	709.5(5)	2.406	73	84	81	72	78
404	6.975(2)	16.976(9)	715.2(4)	2.434	52	56	60	43	53
455	6.986(3)	16.87(2)	712.9(8)	2.415	64	73	68	60	66
457	6.976(3)	16.86(1)	710.6(7)	2.417	65	74	77	62	70
458A	6.984(2)	16.853(7)	711.9(4)	2.413	65	75	72	63	69
Δ	0.015(2)	0.20(1)	6.0(6)	0.033	25	32	22	33	28

Natroalunite contents (i.e., Na) were determined by c_0 parameter variation diagram (Parker, 1962; marked as "1"), equations by c_0 and V_0 parameters (Stoffregen and Alpers, 1992; marked as "2" and "3", respectively) and equations by c_0 parameters (Morrison et al., 2018; marked as "4")

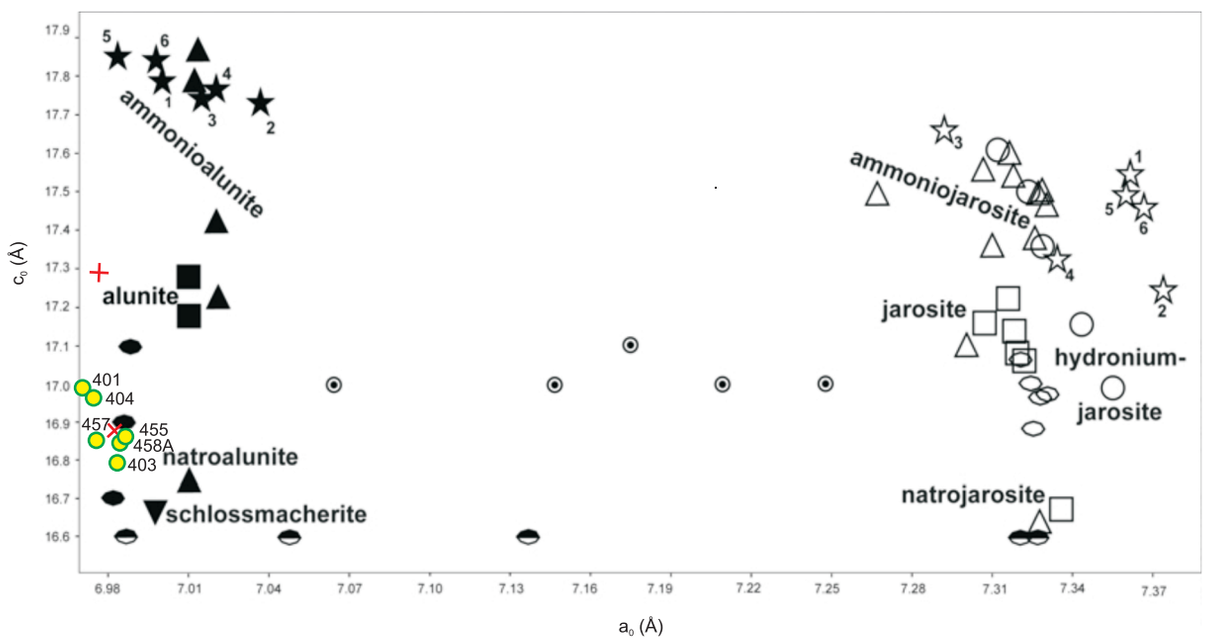

Fig. 5. The alunite samples investigated (yellow-green) as a function of the a_0 unit-cell parameter *versus* c_0 unit-cell parameter (Table 1) juxtaposed onto the inset taken from Parafiniuk and Kruszewski (2010: fig. 5 and references therein)

Symbols "+" and "×" (in red) denote alunite {a_0 = 6.976(1)Å; c_0 =17.295(6)Å; V_0 = 729.0(3)Å^3; c_0/a_0 = 2.479; $[K_{0.83}(H_3O)^+_{0.17}]_{\Sigma 1.00}Al_{3.00}(S_{0.99}O_4)_2(OH)_6$] and natroalunite {$a_0$ = 6.981(1)Å; c_0 = 16.884(6)Å; V_0 = 712.6(3)Å^3; c_0/a_0 = 2.419; $[Na_{0.50}K_{0.38}(H_3O)^+_{0.12}]_{\Sigma 1.00}(Al_{2.95}Fe_{0.13})_{\Sigma 3.08}(S_{0.99}O_4)_2(OH)_6$}, respectively (Tančić and Janežić, 2004)

According to the calculated unit cell dimensions, it is evident that minerals having the alunite group constituents belong to the area between alunite, natroalunite, and schlossmacherite. Also, calculated cell dimensions are at a considerable distance from those of ammonioalunite, ammoniojarosite, jarosite, hydronium-jarosite, and natrojarosite (Figs. 5 and 6). Comparable unit cell dimensions have internal differences (Δ) ranging between the lowermost and the highest values of a_0, c_0, V_0 and ratio c_0/a_0 of 0.015(2), 0.20(1), 6.0(6), and 0.033, respectively; these differences refer mainly to the samples 401 and 403. By using the variation diagram by Brophy et al. (1962), it appears that the samples investigated, according to the a_0 axes, can be classified exclusively to the alunite part, excluding (or insignificant) jarosite (i.e., Fe^{3+}) substitutions for Al^{3+}. On the other hand, their c_0 axes cross beyond the lowest limits, strongly indicating a K^+-Na^+ substitution toward natroalunites. Moreover, by using the variation diagram of Parker (1962), the samples according to the a_0 axes are classified to the alunite-natroalunite group, corroborating the observations. The c_0 axes allowed a more precise determination of their compositions. Accordingly, a single sample (401) should be preliminarily treated as alunite, whereas others should be classified as natroalunites having more or less different compositions. Samples with similar content are 401 and 404; and 455, 457, and 458A. The last three samples have properties very similar to those of the natroalunites that were characterized in earlier studies (Tančić and Janežić, 2004 and the sample T-2 in Drouet et al., 2004). However, the equations of c_0 and V_0 parameters (Stoffregen and

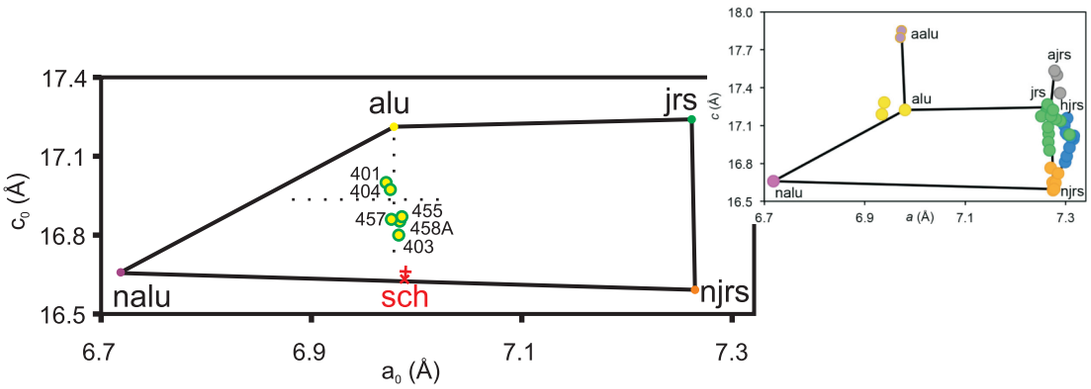

Fig. 6. The alunite samples investigated (yellow-green) as a function of the a_0 unit-cell parameter *versus* c_0 unit-cell parameter (Table 1) juxtaposed onto the alunite (alu)–natroalunite (nalu)–jarosite (jrs)–natrojarosite (njrs) quadrilateral compositions. Inset is taken from Morrison et al. (2018: fig. 9), presented at the upper-right part of the figure

Symbols "+" and "×" (in red) denote schlossmacherite by Schmetzer et al. (1980) and natroalunite by Drouet et al. (2004; sample H-3), respectively

Alpers, 1992) show elevated 4–11 and 4–12 mol.% of the natroalunite contents, respectively. On the other hand, the equations of c_0 parameters (Morrison et al., 2018) show lower 1–9 mol.% of the natroalunite contents. The disagreement influencing the unit cell parameters may be induced by different water contents (Parker, 1962) affecting the crystal structure (distances, angles, polyhedron distortions, sites shifts, etc.). The crystal structure could be affected in various crystallographic directions (i.e., in this case, towards a_0 or c_0) comparable with some other solid solutions (Tančić et al., 2012, 2020). Namely, a certain part of the Na^+ concentration could be substituted by $(H_3O)^+$, because of the very similar ionic ratios of 0.95 and 0.99Å, respectively (Shannon and Prewitt, 1969). Although this substitution has been difficult to document (because it cannot be determined directly by wet-chemistry or electron microprobe analysis-EMPA methods), it has been inferred for most of the samples by accounting for a deficiency in alkalis and an excess of water, compared with the stoichiometric composition. The non-stoichiometric water is generally attributed to the presence of hydronium, nevertheless, it may also reflect other forms of "excess water", as discussed by Ripmeester et al. (1986), Stoffregen et al. (2000), Drouet et al. (2004), Parafiniuk and Kruszewski (2010). With increasing temperature, water contents decrease.

To recheck the compositions of the samples chosen and the alunite minerals characterized (Table 1), we used chemical analyses by applying the appropriate chemical elements (Appendix 2). The results are mostly in agreement with the qualitative and semi-quantitative mineral compositions (Appendix 1), i.e., the SiO_2 content obviously reflects the major quartz, kaolinite, and tridymite previously noted, whereas significant contents of K_2O, Na_2O, Al_2O_3, Fe_2O_3, SO_3 and H_2O^+ confirm the presence of major alunite minerals. On the other hand, CaO, MgO and FeO contents are minor, indicating that no other major mineral phases account for the elements characterized and observed. However, the calculated number of atoms per formula unit (apfu) slightly deviates from the ideal stoichiometric composition. We provide the following explanations, which include the resulting characterization of minor minerals (from ore microscopy):

1. Significant excess of Al and O (sample 401) and H (including sample 457) marks the major kaolinite already characterized. On the other hand, an insignificant increase in Al, O, H and K indicates previously undetected minor illite-sericite content in sample 404;

2. Deficit of H, excess of Fe, higher SO_3/H_2O^+ and lower (Na+K+H)/S (ideal value of 3.5) ratios were caused by pyrite determined in samples 401, 403, 455, and 458A;

3. Excess of Fe in all of the samples is also caused by the characterized minor presence of goethite and/or hematite and/or magnetite;

4. Excess of K (with Ca) indicates a previously undetected minor feldspar content present across the entire set of samples analysed;

5. Deficit between 1 and sum of the calculated (K+Na) contents at the *A* site indicate a variety of substitutions with $(H_3O)^+$ across the entire set of samples analysed. Accordingly, the highest schlossmacherite content is in sample 403, and the lowermost in sample 401.

Despite the resulting unit cell dimensions (Table 1; Figs. 5 and 6) strongly indicating that the ammonium (NH_4^+) contents (at the *A* site) should be minor or negligible (accounting for its larger ionic ratio than K^+ of 1.46Å *versus* 1.33Å, respectively; Shannon and Prewitt, 1969), such a possibility should be cross-checked in future instances (by EMPA, DTA/TGA, FTIR, etc.). An additional validation attempt may indicate the presence of sour-gas-bearing hydrothermal systems (Parafiniuk and

Table 2

Calculated compositions of the minerals studied from the alunite group [in mol. %]

	401	403	404	455	457	458A
Alunite (Alu)	52	27	48	36	35	35
Natroalunite (Nal)	43	27	40	31	48	44
Schlossmacherite (Sch)	5	46	12	33	17	21

Kruszewski, 2010). Moreover, the potential presence of other elements and site vacancies (Drouet et al., 2004) has also not been excluded.

Nevertheless, synthesis of the data assembled (Table 1 and Appendix 2) yields alunite (Alu), natroalunite (Nal), and schlossmacherite (Sch) contents (Table 2). Accordingly, the resulting minerals should be considered as the following solid solutions: $Alu_{52}Nal_{43}Sch_5$ (401), $Alu_{48}Nal_{40}Sch_{12}$ (404), $Nal_{48}Alu_{35}Sch_{17}$ (457), $Nal_{44}Alu_{35}Sch_{21}$ (458A), $Alu_{36}Sch_{33}Nal_{31}$ (455), and $Sch_{46}Alu_{27}Nal_{27}$ (403). A voluminous hydronium content in samples 403, 455 and 458A (Table 2) can for argument be explained as a significant increase of a_0 values by comparison with the other three samples (Table 1; Figs. 5 and 6). Namely, such a substitution causes an increase of this crystallographic parameter (Parker, 1962; Stoffregen and Alpers, 1992; Stoffregen et al., 2000). In addition, the substitution influenced the other two parameters (c_0 and V_0) considering the different values among the computed natroalunite content (marks 1–4 at Table 1). Epithermal environments account for significant gold production (Poulsen et al., 2000; Tosdal et al., 2009; Walshe and Cleverley, 2009). Because alunites are a well-recognized indicator for gold in epithermal environments, this element has also been analysed. Contents of Au are mostly at insignificant levels, i.e., below the detection limit (Appendix 2). There is only a single higher value (0.4 ppm) determined in sample 401. Such a value might be interesting for economic evaluations because the mean value in the neighbouring Lece ore-field is 0.03 ppm (from 0.004 to 5.03 ppm; Stajević, 2004).

DISCUSSION

The mineralogical data obtained show that the complex investigated underwent processes of hydrothermal alteration. Straightforward identification of outcrop-scale intense changes within the rocks demonstrates argillization and silicification. Limonitization is a relatively common occurrence, whereas sericitization, chloritization, and hematitization show only local appearances (Fig. 4). The petrography results corroborated the presence of slightly to completely altered volcanic and pyroclastic rocks of andesitic, andesitic-dacitic, and dacitic composition, consistent with detailed field sampling (Fig. 3). Recorded alterations are argillization, silicification, sericitization, opacitization, chloritization and limonitization. Occasionally some occurrences of carbonatization and epidotization were recorded. Similarly, the XRPD mineral compositions (Appendix 1) attest to the presence of alteration within the samples investigated. Silicification and kaolinization are the most frequent; sericitization is limited, whereas limonitization (of goethite-type), chloritization, and hematitization are minor. The method additionally allowed the characterization of other kinds of alteration and of secondary minerals, such as the alunite group minerals, various clay minerals, zeolites, diaspore, etc. The presence of quartz, alunite, pyrophyllite, kaolinite (dickite), illite, and pyrite (also with an absence of calcite and adularia in this paragenesis) indicates high-sulfidation and advanced or progressive argillic alteration (Sillitoe, 1993; White and Hedenquist, 1995; Taylor, 2007).

The mineral composition (Appendix 1) further permits the classification of regions with similar mineral contents. Such grouping allows the designation of a specific mineral cluster/group to an alteration zone (Fig. 3). Importantly, such extrapolation into a group of similar minerals may facilitate the correlation of the prospective mineralization types. The correlation allows extrapolation plus detailed interpretation despite the difference in rock lithostratigraphic properties (the range of geological units; Fig. 3). For example, samples with documented mineralization involving the alunite group were collected from variably hydrothermally altered geological units comprising:

- andesitic pyroclastic rocks;
- hornblende andesites;
- secondary quartzites;
- pyroxene andesites.

The extrapolation and correlation of the alunite mineral groups show that structure and lithology were the primary controls on the emplacement of the alunite mineralization. There is a close correspondence between the five regions/alteration zones of the alunite mineralization and their distinct mineralogical properties, as shown in Table 3.

Our results show that advanced argillic alteration is most intense at the Žuta Bara (I) region with 8 natroalunite, 1 jarosite, 22 kaolinite-dickite, 8 illite-sericite, and 2 pyrite occurrences; including the documented presence of pyrophyllite and diaspore minerals (both with 7 occurrences). The Prolom (II) region, with nine different minerals of the alunite group characterized, and 6 kaolinite-dickite, 4 illite-sericite, and 2 pyrite occurrences, is less argillized. On the other hand, the regions Đake (III, 6 alunites) and Banjska Reka (IV, 3 jarosites) also have a documented

Table 3

Data comparing five separate alunite-bearing regions

Region/zone	Rocks alterations	Mineral compositions with number of occurrences								LC	FF
	Slight	Intensive	Alunite group minerals	Sm	K	I	P	D	Py		
I Žuta Bara	1	21	NA (8), J (1)	2	22	8	7	7	2	2	>100
II Prolom	n.d.	8	NA (3), J (3), A (2), NJ (1)	9	6	4	n.d.	n.d.	2	11	>100–40
III Đake	3	n.d.	A (6)	n.d.	n.d.	5			n.d.	n.d.	>100–40
IV Banjska Reka	n.d.	2	J (3)	n.d.		3			1		>100–40
V Prolomska Reka*	1	2	A (4)	8		1			n.d.		n.d.

Symbols are the same as in Appendix 1; LC – low crystallinity of minerals; FF – frequency of fractures (in F/m^2, after Hrković, 1991); numbers of total (major and minor) occurrences are also show; * – together with the Mehanski Potok locality (1 alunite occurrence); n.d.– not detected

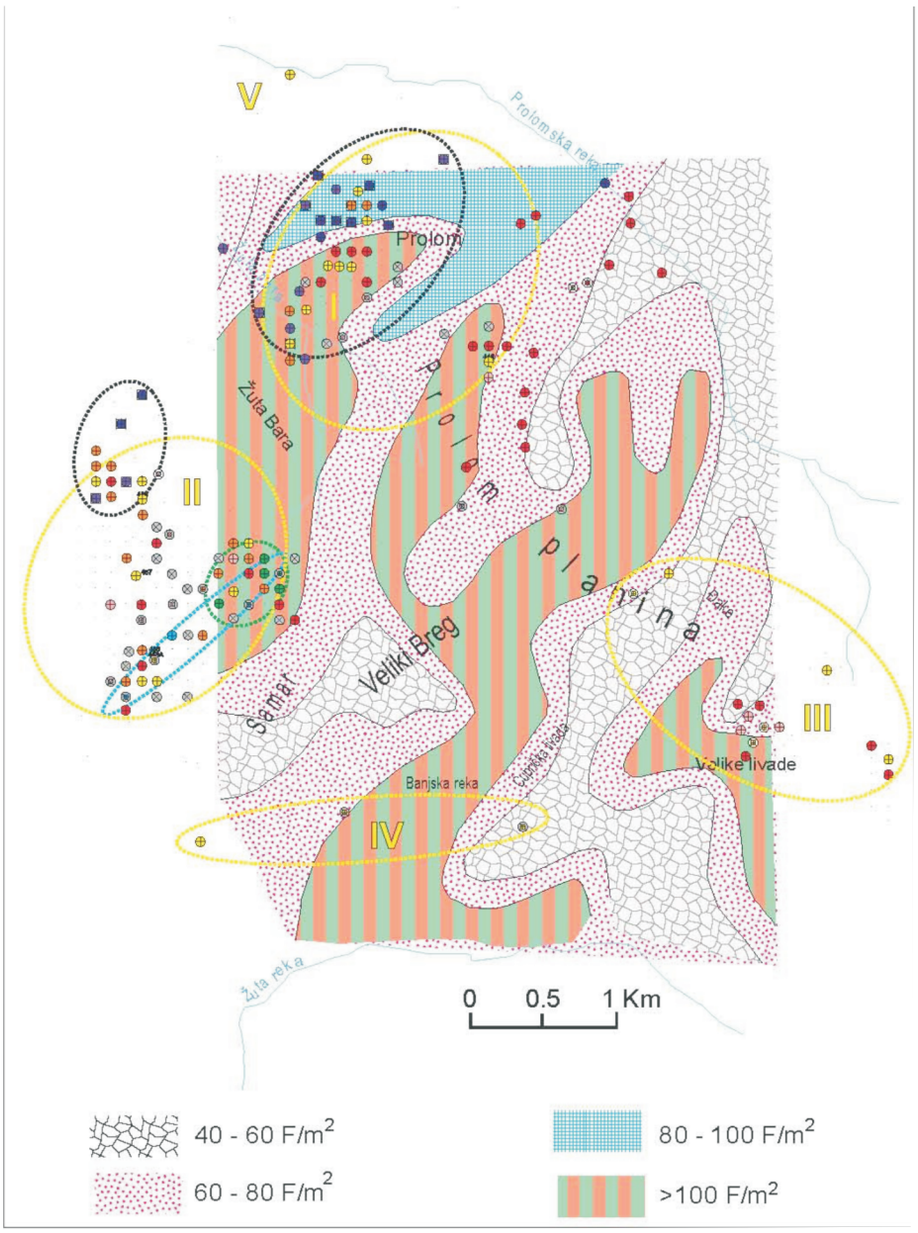

Fig. 7. The density of microfractures juxtaposed onto the here isolated mineral regions (Fig. 3 and Table 3)

I – Žuta Bara, II – Prolom, III – Đake, IV – Banjska Reka;
inset is taken from Hrković (1991: fig. 5)

presence of illite-sericite, though without kaolinite or smectite detected; whereas the Prolomska Reka region (V, 3 alunites) has a considerable number of the smectite occurrences. The regions I–IV are also mutually correlative and data from them fits well with the frequency of fractures, i.e., the recorded petrophysical anomalies exposed by previous geophysical surveys at the Žuta Bara-Raskrsnice, Samar, Ćuprića Livada, and Velike Livade localities (Hrković, 1991; Fig. 7). Despite the study area spanning a large surface area, it is obvious that the degree of alteration decreases with the frequency of the fractures from Žuta Bara, over Prolom, to the Đake and Banjska Reka regions (Table 3).

Although exploring the precise ore-forming processes associated with this volcanic-hydrothermal environment are beyond this paper's scope, the resulting minerals and mineral associations, including the differences recorded across the alteration zones investigated, indicate a near-surface hydrothermal environment, characterized by rapidly changing emplacement conditions. The estimated formation temperatures, based on mineralogical geothermometers, indicate a wide temperature range, starting from the highest at >1470°C (β-cristobalite) and/or >870°C (β-tridymite) decreasing to ≤80°C (Lece ore field; sphalerite geothermometer; Tančić, 2017, 2018). We presume that the palaeotemperature most probably decreased

from the initial or primary magmatic activity (forming volcanic rocks) towards the younger, low hydrothermal (epithermal), and other variously altered regions. Many alteration minerals are stable over limited temperature and/or pH ranges, thus providing important information for reconstructing the thermal and geochemical structure of a hydrothermal system (Reyes, 1990; White and Hedenquist, 1995). For example, among the five separate alunite-bearing regions, the formation temperatures at the Đake region should have been >220°C (according to the illite-sericite observed). In addition to these principal regions, it is also possible to delineate other temperature variations considering different rock and mineral clusters/groups. Significant temperature variations have been recorded among the same mineral-based area/region. Consequently, the observed variations are indicators of the array of sub(mineralogical)-zones introduced here. At the LC zone of the Žuta Bara region (Fig. 3), natroalunite and jarosite (<100°C), β-cristobalite and β-tridymite (100–160°C) and smectite (<160°C) occurrences are in proximity to (several hundred metres from) occurrences with pyrophyllite (200–300°C), diaspore (>150°C) and illite (220–300°C). Similar constraints can be attributed to the Prolom (natroalunite, jarosite, β-cristobalite, β-tridymite and smectite versus illite), Banjska Reka (jarosite *versus* illite), and Prolomska Reka (smectite *versus* illite) regions. Alunite occurs at <320°C, kaolinite at <200°C, whereas the appearance of dickite is at the 120–280°C range. The resulting synthesis indicates that the altered regions have formed in a temperature range from <100 to ~300°C, consistent with epithermal type palaeoenvironments.

The documented presence of the schlossmacherite components in the Žuta Bara and Prolom regions (Tables 1 and 2; Figs. 5 and 6) further corroborates the presence of a low-temperature environment, while the total mineral content provides more specific temperature constraints (temperature increases from sample 403 to samples 401 and 404). The presence of primary cristobalite or tridymite (from high-temperature devitrification of volcanic glass) indicates the rocks least affected in space and time by low-temperature hydrothermal fluids (Izawa et al., 1990). This is in agreement with the presumption that the epithermal deposits are younger than their enclosing rocks (Taylor, 2007).

Other parameters, such as pressure, pH, Eh, etc., affect the estimates of the origin variations. For example, the minerals from the alunite group documented and their parageneses (i.e., kaolinite-dickite, pyrophyllite, and diaspore) reflect the activity of highly-acidic hydrothermal fluids, marked by pH values ranging from <2 to ≥5 (Giggenbach, 1992). However, the presence of smectite (which forms in a neutral pH environment; Reyes, 1990; White and Hedenquist, 1995) among the Žuta Bara, Prolom, and Prolomska Reka alunite-bearing regions rather typify a multi-staged history of alteration preserved within each particular host rock. The results thus demonstrate a recurrent activity of regional palaeohydrothermal systems. Furthermore, the pH values support a hypothesis of $(H_3O)^+/(Na, K)^+$ exchange, with the highest schlossmacherite content documented in sample 403. From the correlations (Fig. 8) between the measured pH values (Appendix 2) within the computed alunite, natroalunite and schlossmacherite components (Table 2), it could be observed that the positive coefficient of the regression (R^2) and the high correlation coefficients (r) can be associated with the alunite and natroalunite contents (r = 0.80 and r = 0.62, respectively). On the other hand, a high negative correlation coefficient (r = –0.84) is observed between the pH and schlossmacherite contents. The main reason for such dependency could be that, unlike alunite or natroalunite, schlossmacherite has a covalent bond between S-O-H atoms. In aqueous solution, this group acts as an acid, and releases the H^+ ion. The final result is a higher concentration of $(H_3O)^+$ ions (lower pH) once schlossmacherite is present. We strongly believe that the pH values in samples 401 and 457 should be higher according to the determined schlossmacherite component; however, it seems that these values were slightly decreased due to a minor presence of kaolinite.

CONCLUSIONS

This detailed mineralogy-based study (lithogeochemical prospecting, petrography, XRPD, unit cell dimensions, chemical analyses, ore microscopy, pH) of the Lece-Radan volcanic complex shows that acidic hydrothermally-driven fluid flow was powered by magma upwelling. The Neogene volcanic episode led to a range of alteration types, including the precipitation of the alunite mineral group, pyrophyllite, quartz, diaspore, kaolinite (dickite), and illite. This process typifies fluid-dominated near-surface conditions (epithermal environment), in-

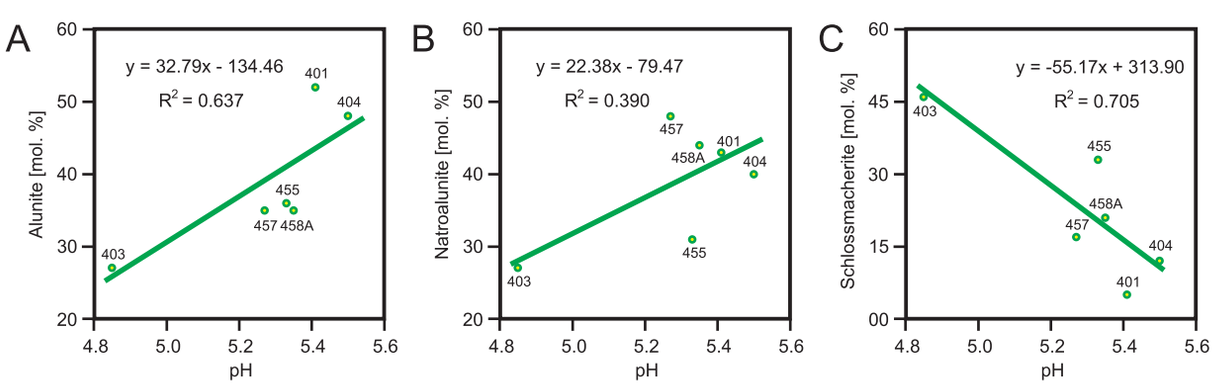

Fig. 8. Diagrams exposing variations in pH values from:
A – alunite, B – natroalunite, C – schlossmacherite contents

cluding advanced argillic alteration as an important indicator (Sillitoe, 1993; Tosdal et al., 2009). The host rocks were exposed to hydrothermal fluids, primarily by replacement (i.e., by solution and reprecipitation) or by open-space filling (e.g., veins, breccias, pore spaces). The deposits originating by the open-space filling mechanism typically reflect structurally-controlled flow of hydrothermal fluids (planar *versus* irregular fractures, etc.). The deposition of the alunite-bearing mineral group precipitated closely corresponds with the zones of higher fracture frequency (Table 3 and Fig. 7). The resulting mineralogical zoning (Fig. 3) demonstrates the importance of the structural setting for the origin of the mineralization types characterized.

Minerals from the alunite group were documented for the first time in the following localities of the volcanic complex: Žuta Bara (9 occurrences), Prolom (9 occurrences), and Đake, Banjska Reka, and Prolomska Reka (total 13 occurrences). Samples with alunitization collected from different hydrothermally-changed geological units of different ages indicate that structural and lithological control factors were of critical importance for their deposition/precipitation. The minerals from the alunite group have different compositions, corresponding with the unit cell dimensions, pH values (Tables 1, 2 and Figs. 5, 6, 8) and surface-exposed host rocks (Fig. 3). Their documented presence may link the epithermal-type ores (determined temperatures from <100 to ~300°C) with the high-sulphidation style of the Lece-Radan volcanic massif. However, extensional lithospheric-scale Neogene tectonism above a precursor Neotethyan convergent margin represents an atypical setting for the Late Oligocene-Miocene magma sourcing. Such an atypical palaeotectonic environment accounting for epithermal ores requires further investigation.

This study shows that in addition to alunite, the smectite, kaolinite-dickite, and pyrophyllite mineral groups might be of economic interest, helpful to additional exploration. The documented presence of diaspore has also been of significant impact because this mineral is rare in Serbia. The nearest well-documented presence of diaspore (-boehmite) are the bauxites of Grebnik Mt. (~100 km to the south-west; Cvetković and Tančić, 2019).

Acknowledgments. This research did not receive any specific grant from funding agencies in public, commercial or not-for-profit sectors. The authors are grateful to S. Dušanić for useful expert advice; Ž. Cvetković for the ore microscopy analysis; and to D. Radovanović and T. Sekulić for their technical assistance. The authors are also grateful to T. Bajda and four anonymous reviewers for their constructive reviews and valuable suggestions that greatly improved the initial version of the manuscript.

REFERENCES

Bayliss, P., Kolitsch, U., Nickel, E.H., Pring, A., 2010. Alunite supergroup: recommended nomenclature. Mineralogical Magazine, **74**: 919–927.

Brophy, G.P., Sheridan, M.F., 1965. Sulfate studies IV: the jarosite-natrojarosite-hydronium jarosite solid solution series. American Mineralogist, **50**: 1595–1607.

Brophy, G.P., Scott, E.S., Snellgrove, R.A., 1962. Sulfate studies II: solid solution between alunite and jarosite. American Mineralogist, **47**: 112–126.

Cvetković, Ž., Tančić, P., 2019. Mineralogical and crystallographic characteristics of bauxites from some Grebnik's (Metohija, Serbia) ore deposits. Geološki anali Balkanskoga poluostrva, **80**: 45–61.

Dimitrijević, M.D., 1997. Geology of Yugoslavia. Geological Institute-Gemini, Special Publication, Barex, Belgrade.

Dimitrijević, M., Grubić, A., 1977. Models of geotectonic development of the northeastern Mediterranean. In: Metallogeny and Plate Tectonics in the Northeast Mediterranean (ed. S. Janković): 21–103. Faculty of Mining and Geology, University of Belgrade.

Drouet, C., Pass, K.L., Baron, D., Draucker, S., Navrotsky, A., 2004. Thermochemistry of jarosite-alunite and natrojarosite-natroalunite solid solutions. Geochimica et Cosmochimica Acta, **68**: 2197–2205.

Garvey, R., 1987. Least-square unit cell refinement, Version 86,2. Department of Chemistry, North Dakota State University.

Giggenbach, W.F., 1992. Magma degassing and mineral deposition in hydrothermal systems along convergent plate boundaries. Economic Geology, **87**: 1927–1944.

Hendricks, S.B., 1937. The crystal structure of alunite and jarosites. American Mineralogist, **22**: 773–784.

Hrković, K., 1991. Structural-petrophysic-metallogenic features of non-ferrous deposits in Yugoslavia as a criterion for prognosis (in Serbian with English summary). Rudarsko-geološki fakultet, Katedra ekonomske geologije, Beograd.

Ilić, M., 1961. O pojavama alunitskih stena na Majdanu iznad Boljetina kod Kosovske Mitrovice (in Serbian). Zbornik radova RGF, **8**: 19–36.

Izawa, E., Urashima, Y., Ibaraki, K., Suzuki, R., Yokoyama, T., Kawasaki, K., Koga, A., Taguchi, S., 1990. The Hishikari gold deposit: high-grade epithermal veins in Quaternary volcanics of southern Kyushu, Japan. Journal of Geochemical Exploration, **36**: 1–56.

Janković, S., 1977. Major Alpine ore deposits and metallogenic units in the northeastern Mediterranean and concepts of plate tectonics. In: Metallogeny and Plate Tectonics in the NE Mediterranean: 105–171. Faculty of Mining and Geology, University of Belgrade.

Janković, S., 1990. The ore deposits of Serbia: regional metallogenic settings, environments of deposition, and types (in Serbian with English summary). Rudarsko-geološki fakultet, Beograd.

Jelenković, R., 1998. Gold mineralizations in the western part of the Bor metallogenic zone (East Serbian sector of the Carpatho-Balkan metallogenic province). XVI Congress of the Carpathian-Balkan Geological Association, Vienna, August 30th to September 2nd.

Jelenković, R., Kostić, A., Životić, D., Ercegovac, M., 2008. Mineral resources of Serbia. Geologica Carpathica, **59**: 345–361.

Joksimović, D., 1970. Izveštaj o regionalnim istraživanjima mineralnih sirovina Kopaoničke oblasti u 1970. godini (in Serbian). Unpubl. report, Geological Institute, Beograd.

Malešević, M., Vukanović, M., Branković, T., Obradović, Z., Karajičić, Lj., Dimitrijević, M.D., Urošević, M., Stanisavljević, R., 1979. Osnovna geološka karta SFRJ 1:100 000 – list Kuršumlija (in Serbian). Savezni geološki zavod, Beograd.

Marović, M., Toljić, M., Rundić, Lj., Milivojević, J., 2007. Neoalpine Tectonics of Serbia. Serbian Geological Society.

Menchetti, S., Sabelli, C., 1976. Crystal chemistry of the alunite series: crystal structure refinement of alunite and synthetic jarosite. Neues Jahrbuch für Mineralogie Monatshefte, (9): 406–417.

Monthel, J., Vadala, P., Leistel, J.M., Cottard, F., with the collaboration of Ilic, M., Strumberger, A., Tosovic, R., Stepanovic, A., 2002. Mineral deposits and mining districts of Serbia. Compilation map and GIS databases. BRGM/RC-51448-FR.

Morrison, S.M., Downs, R.T., Blake, D.F., Prabhu, A., Eleish, A., Vaniman, D.T., Ming, D.W., Rampe, E.B., Hazen, R.M., Achilles, C.N., Treiman, A.H., Yen, A.S., Morris, R.V., Bristow, T.F., Chipera, S.J., Sarrazin, P.C., Fendrich, K.V., Morookian, J.M., Farmer, J.D., Des Marais, D.J., Craig, P.I., 2018. Relationships between unit-cell parameters and composition for rock-forming minerals on Earth, Mars, and other extraterrestrial bodies. American Mineralogist, **103**: 848–856.

Parker, R.L., 1962. Isomorphous substitution in natural and synthetic alunite. American Mineralogist, **47**: 127–136.

Parafiniuk, J., Kruszewski, Ł., 2010. Minerals of the ammonioalunite-ammoniojarosite series formed on a burning coal dumps at Czerwionka, Upper Silesian Coal Basin, Poland. Mineralogical Magazine, **74**: 731–745.

Poulsen, K.H., Robert, F., Dubé, B., 2000. Geological classification of Canadian gold deposits. Geological Survey of Canada Bulletin, **540**: 1–106.

Reyes, A.G., 1990. Petrology of Philippine geothermal systems and the application of alteration mineralogy to their assessment. Journal of Volcanology and Geothermal Research, **43**: 279–309.

Ripmeester, J.A., Ratcliffe, C.I., Dutrizac, J.E., Jambor, J.L., 1986. Hydronium ion in the alunite-jarosite group. Canadian Mineralogist, **24**: 435–447.

Schmetzer, K., Ottemann, J., Bank, H., 1980. Schlossmacherite, $(H_3O,Ca)Al_3[(OH)_6((S,As)O_4)_2]$, ein neues Mineral der Alunit-Jarosit-Reihe. Neues Jahrbuch für Mineralogie, Monatshefte: 215–222.

Schmid, S.M., Bernoulli, D., Fügenschuh, B., Georgiev, N., Kounov, A., Maţenco, L., Oberhänsli, R., Pleuger, J., Schefer, S., Schuster, R., Tomljenović, B., Ustaszewski, K., van Hinsbergen, D.J.J., 2020. Tectonic units of the Alpine collision zone between Eastern Alps and Western Turkey. Gondwana Research, **78**: 308–374.

Shannon, R.D., Prewitt, C.T., 1969. Effective ionic radii in oxides and fluorides. Acta Crystallographica, **B25**: 925–946.

Sillitoe, R.H., 1993. Epithermal models: genetic types, geometrical controls and shallow features. Geological Association of Canada, Special Paper, **40**: 403–417.

Spahić, D., Gaudenyi, T., 2019. Intraoceanic subduction model of northwestern Neotethys and geodynamic interaction with Serbo-Macedonian foreland: descending vs. overriding near-trench dynamic constraints (East Vardar Zone, Jastrebac Mts., Serbia). Geološki anali Balkanskog poluostrva, **80**: 65-85.

Spahić, D., Gaudenyi, T., 2020. 60 years of the Serbo-Macedonian Unit concept: From Cadomian towards Alpine tectonic frameworks. Geološki anali Balkanskoga poluostrva, **81**: 41–46.

Stajević, B., 2004. Geochemical haloes of gold in the Lece ore field (southern Serbia). Geološki anali Balkanskoga poluostrva, **65**: 93–99.

Stoffregen, R.E., Alpers, C.N., 1992. Observations on the unit cell parameters, water contents and δD of natural and synthetic alunites. American Mineralogist, **77**: 1092–1098.

Stoffregen, R.E., Alpers, C.N., Jambor, J.L., 2000. Alunite-jarosite crystallography, thermodynamics and geochronology. Reviews in Mineralogy and Geochemistry**, 40**: 453–479.

Tančić, P., 2017. Comparison of the crystallographic-chemical characteristics of sphalerites from the Kiževak ore deposit with some other deposits. Part I: Preliminary reconsideration about their formation conditions. Bulletin of Mines, **114**: 101–117.

Tančić, P., 2018. Comparison of the crystallographic-chemical characteristics of sphalerites from the Kiževak ore deposit with some other deposits. Part II: Construction of the four-component a_0-FeS-P-T diagram (option I) and determination of the formation conditions. Bulletin of Mines, **115**: 59–73.

Tančić, P., Janežić, V., 2004. Crystallographicaly-mineralogical characteristics of alunite and natroalunite from Veliki Bukovik near Raška. Bulletin of Geoinstitute, **39**: 155–167.

Tančić, P., Dimitrijević, R., Poznanović, M., Pačevski, A., Sudar, S., 2012. Crystal structure and chemical composition of ludwigite from Vranovac ore deposit (Boranja Mountain, Serbia). Acta Geologica Sinica, **86**: 1524–1538.

Tančić, P., Kremenović, A., Vulić, P., 2020. Structural dissymmetrization of optically anisotropic $Grs_{64\pm1}Adr_{36\pm1}Sps_2$ grandite from Meka Presedla (Kopaonik Mt., Serbia). Powder Diffraction, **35**: 7–16.

Taylor, B.E., 2007. Epithermal gold deposits. Geological Association of Canada, Mineral Deposits Division, Special Publication, **5**: 113–139.

Tosdal, R.M., Dilles, J.H., Cooke, D.R., 2009. From source to sinks in auriferous magmatic-hydrothermal porphyry and epithermal deposits. Elements, **5**: 289–295.

Tućan, F., 1938. Sanidinski daciti Zvečana i Sokolice i alunitska stena od Boljetina (Majdan) kod K. Mitrovice (in Serbian). Rad JAZU, **261**.

Vasić, I., 1986. Izveštaj o istraživanju alunita u sektoru Biočina kod Raške (in Serbian). Unpubl. report, Republički SIZ za geološka istraživanja, Beograd.

Vukanović, M., Dimitrijević, M.D., Dimitrijević, M.N., Karajičić, Lj., Rajčević, D., Navala, M., Urošević, M., Malešević, M., Trifunović, S., Serdar, R., Atin, B., 1982. Osnovna geološka karta SFRJ 1:100 000 – list Podujevo (in Serbian). Savezni geološki zavod, Beograd.

Vukašinović, **S**., **1973.** Prilog geotektonskoj reonizaciji međugraničnog prostora Dinarida, Panonida i Srpsko-makedonske mase (in Serbian). Zapisnici SGD za 1972. godinu: 1–18.

Walshe, J.L., Cleverley, J.S., 2009. Gold deposits; where, when and why. Elements, **5**: 288.

White, N.C., Hedenquist, J.W., 1995. Epithermal gold deposits: styles, characteristics and exploration. SEG Newsletter, **23**: 9–13.

Wang, R., Bradley, W.F., Steinfink, H., 1965. The crystal structure of alunite. Acta Crystallographica, **18**: 249–252.